World Journal of Advanced Research and Reviews
eISSN: 2581-9615 CODEN (USA): WJARAI
Cross Ref DOI: 10.30574/wjarr
Journal homepage: https://wjarr.com/

(RESEARCH ARTICLE)

Check for updates

Study of Biosynthesis of Zinc Oxide Nanoparticles Using *Issatchenkia orientalis*, its Characterization and Application as Antimicrobial and Photocatalytic Agent

Anuradha S. Pendse *, Sayyed Iqra Naaz Aagar Ali and Tejashree Shivram Phepade

Department of Microbiology, Wilson College, Mumbai 400007

World Journal of Advanced Research and Reviews, 2026, 29(01), 042-053

Publication history: Received on 27 October 2025; revised on 26 December 2025; accepted on 29 December 2025

Article DOI: https://doi.org/10.30574/wjarr.2026.29.1.4069

Abstract

Nanoparticles (NPs) exhibit unique physicochemical properties due to their nanoscale dimensions and structural characteristics. In recent years, nanotechnology has transformed the scientific and industrial research. In the present study, we investigated the potential of yeast strains in bio-synthesis of Zinc Oxide nanoparticles (ZnO NPs). Further, we characterized the obtained NPs and evaluated its antimicrobial and photocatalytic potential. The isolates were screened from soil, sea water and bagasse samples, and the most potential isolate was identified as *Issatchenkia orientalis* based on molecular sequencing. Among the seven isolates obtained in this study, only *I. orientalis* formed ZnO NPs. Optimum yield of NPs was obtained at room temperature, when the media was supplemented with culture density of 0.8 $O.D_{540nm}$ and 6% inoculum size, and 60mM $ZnSO_4$. The NPs were characterized using UV–Vis spectroscopy, FTIR, SEM and particle size analysis. It showed characteristic peaks at 370nm and 380nm in UV-Vis spectroscopy, and between 400 and 700cm^{-1} in FTIR analysis. The average size detected was 843.9nm, indicating that the formed particles were nano-clusters. SEM analysis further confirmed the biosynthesis of irregular NPs. The NPs showed moderate antibacterial activity, with maximum efficacy observed against *Bacillus subtilis.* The NPs were also capable of photocatalytic degradation of Congo red dye, which is a toxic industrial pollutant. A degradation efficiency of 54.68% was achieved within 120 mins. Overall, this study demonstrates controlled bio-synthesis of ZnO NPs and paves the way for developing efficient and sustainable solutions for environmental and biomedical applications.

Keywords: Bio-synthesis; Nanoparticles; Nano-clusters Issatchenkia orientalis; FTIR; SEM

1. Introduction

Nanoparticles (NPs) have attracted significant attention in recent decades due to their diverse and novel magnetic, physicochemical and opto-electronic properties. These properties are strongly influenced by their size and distribution [1]. The extremely small size dimensions of NPs result in a high surface area to volume ratio, which characterizes their unique mechanical, thermal, optical and electrical properties [2]. Presently, NPs are extensively utilized in a wide range of applications including catalysis, pharmaceuticals, biosensors for disease diagnosis, drug delivery systems and photocatalytic processes [3, 4].

The NPs are typically synthesized using various physical and chemical techniques, which are significantly influenced by factors such as temperature, pH, metal ion concentration and interactions between reducing and stabilizing agents [1, 4]. However, despite their efficiency, most conventional synthesis methods use toxic chemicals that pose serious environmental and health hazards. Many organic solvents, reducing agents and stabilizers used in these methods are cytotoxic and carcinogenic [5].

* Corresponding author: Anuradha S. Pendse

To address these concerns, synthesis of NPs using biological entities such as plants, bacteria, fungi, algae or viruses is encouraged under a concept of 'green synthesis'. This approach is a sustainable and eco-friendly alternative to chemical techniques, which utilizes the biochemical machinery of micro-organisms and plants [6]. Biogenic NPs synthesized using the green approach are typically biocompatible, stable and non-toxic, making them ideal for biomedical applications such as antimicrobial agents, and in targeted drug delivery systems [7]. Among the biological routes, plant mediated NP synthesis methods are most popular due to their simplicity, cost-effectiveness and scalability. Plant extracts contain phytochemicals such as flavonoids, polyphenols, terpenoids, alkaloids, amino acids and organic acids which act as reducing, capping and stabilizing agents during nanoparticle formation [8]. Similarly, microorganisms can also serve as efficient biological systems for NP synthesis, through extracellular or intracellular pathways. In microorganisms, the biomolecules such as peptides, proteins and enzymes act as natural capping agents, preventing aggregation and ensuring enhanced NP stability [9]. Various microorganisms have been successfully employed for synthesizing metal NPs. Few examples include extracellular silver and ZnO NPs with antimicrobial activity synthesized using *Pichia fermentans* [10], extracellular spherical ZnO NPs with antimicrobial and photocatalytic activity synthesized using *Serratia nematodiphila* [11] and anisotropic silver NPs with antimicrobial and larvicidal activity synthesized using *Bacillus subtilis* [12].

Zinc oxide nanoparticles (ZnO NPs) are particularly well-documented for a wide range of applications. These NPs exhibit strong inhibitory effects against a broad spectrum of microorganisms, primarily through mechanisms involving the generation of reactive oxygen species, disruption of cell membrane integrity, and release of Zn^{2+} ions [13]. Furthermore, their photocatalytic efficiency under UV light has been demonstrated in the degradation of organic dyes such as Rhodamine B, Congo red, and Methylene blue, making them suitable candidates for environmental remediation applications [14]. ZnO NPs are also employed in wastewater treatment, particularly in the removal of heavy metals and other toxic pollutants through adsorption and photocatalytic oxidation processes [13].

Despite significant progress in biogenic NP synthesis, limited studies have investigated the potential of yeasts in NP synthesis. Considering this research gap, the present study aims to investigate the biosynthesis of ZnO NPs using a yeast strain isolated from bagasse, followed by its yield optimization, characterization and evaluation of antimicrobial and photocatalytic activities.

2. Materials and methods

2.1. Sample Collection

The following samples were collected for isolation of yeast strains with high NP yield potential; (1) surface and rhizospheric soil samples from Wilson college garden, Mumbai, (2) Sea water sample from Girgaum chowpatty, Mumbai, and (3) Bagasse from local sugarcane juice shops in Mumbai. Soil samples were collected in sterile dilution tubes, sea water samples in sterile flasks, while bagasse samples were placed in a sterile Petri plates. All samples were transported to the laboratory and stored in refrigerator until processing.

2.2. Enrichment of Flora from Different Samples

Enrichment of yeasts was done using Sabouraud Dextrose Broth (SDB). It is a selective medium for growing fungi due to its high dextrose content and low pH [15]. Each environmental sample (1mL or 1g) was inoculated into 50 mL sterile SDB and incubated on a rotary shaker at room temperature (30 ± 2°C) for 48 h.

2.3. Isolation and Maintenance of Yeast Isolates

Following the enrichment process, aliquots from the broth cultures were streaked on sterile Sabouraud Dextrose Agar (SDA) plates using the four-quadrant streaking technique. The plates were incubated at room temperature for 48 h. After incubation, the isolated colonies were subjected to monochrome staining using crystal violet to confirm yeast characteristics. Single colonies obtained on SDA plates were maintained on SDA slants, after confirming luxuriant growth and absence of contamination. The cultures were stored at 4°C.

2.4. Enzymatic Profiling of Isolates for Nanoparticle Synthesis

To determine the enzymatic potential of the yeast isolates for NP synthesis, two biochemical assays were performed including nitrate reduction test (to detect nitrate reductase enzyme) and Trimethyl Tetrazolium Chloride (TTC) dye reduction test (to detect dehydrogenase enzyme). For nitrate reduction test, 24 h old yeast isolates grown on SDA slants were washed with sterile phosphate buffered saline (PBS, pH 7.5). The optical density (OD) of the suspension was adjusted to 0.5 at 540 nm using a colorimeter (ELICO CL-63 Photometer). An aliquot of 0.1 mL of each standardized

suspension was inoculated into 2 mL of sterile nitrate peptone water and incubated at room temperature for 24 h. After observing visible growth, 0.5 mL of 0.8% sulphanilic acid and 0.5 mL of 0.5% α-naphthylamine were added. The development of a red coloration (formation of formazan) within a few minutes confirmed nitrate reductase enzyme activity.

To detect dehydrogenase activity, sterile SDA supplemented with 1% TTC (Loba Chemie) was poured into sterile 9 cm Petri plates. The isolates were spot inoculated using a sterile nichrome loop and incubated at room temperature for 24 h. Formation of red coloration around colonies indicated reduction of TTC by dehydrogenase enzymes.

2.5. Biosynthesis of Zinc oxide Nanoparticles

Before synthesizing the ZnO NPs, the Maximum Tolerable Concentration (MTC) of zinc sulphate ($ZnSO_4$) was determined using MTC assay. 1M stock solution (14.377 g in 50 mL distilled water) of $ZnSO_4$ was serially diluted to obtain concentrations between 20 mM to 1000 mM. Sterile 20 mL molten and cooled (40°C) SDA butts were seeded with 0.2 mL of isolates (OD_{540} = 0.5). After mixing, the seeded medium was poured into sterile Petri plates. Once solidified, wells (6 mm diameter) were bored using a sterile cork borer, and 50 µL of each $ZnSO_4$ dilution was added to separate wells. A control well containing 50µL sterile distilled water served as control. Plates were incubated at room temperature for 24 h. The concentration at which colorless inhibition zones were formed after incubation indicated MTC of $ZnSO_4$.

The NPs were synthesized following the method described by Chauhan et al. [16] with some modifications. While the above study employed the culture supernatant of *Pichia fermentans* for NP synthesis, the present study utilized the cell biomass of the potential isolate as the biocatalyst. The isolate density was adjusted to 0.5 at 540 nm and an inoculum size of 2% was inoculated into 50 mL SDB, and incubated under shaking conditions (150 rpm) for 24 h. The culture broth was centrifuged at 5500 rpm for 30 min, and the cell pellet was washed thrice with sterile PBS (pH 7.5). The cell density was adjusted to 0.2 OD_{540} and 1 mL of this suspension was added to 50 mL sterile 60mM $ZnSO_4$ solution (MTC). The mixture was incubated at room temperature for 24 h under shaking conditions. *Saccharomyces cerevisiae* served as a negative control. Post-incubation, the isolate was centrifuged at 1000 rpm for 15 min. The pellet was sequentially washed thrice with deionized water and once with ethanol. It was then dried at 40°C for 24 h to obtain white ZnO NP powder.

2.6. Identification of Potential Isolate

Identification of potential isolate was done based on molecular methods. Freshly isolated yeast culture was submitted to Hi-Media Gx360 Solutions, Hi-Media Laboratories Pvt Ltd, Thane, for Internal Transcribed Spacer (ITS) sequencing. This method targets the internal transcribed spacer regions of ribosomal DNA, which are highly variable and serve as reliable genetic markers for species level identification [17].

2.7. Solubility of Synthesized ZnO Nanoparticles

The solubility of synthesized ZnO NPs was visually assessed in various solvents such as distilled water, methanol, dimethyl sulfoxide, n-hexane, chloroform, cyclohexane, diethyl ether, n-butane, 1 N HCl and 1 N NaOH. Approximately 2 mg of ZnO NPs was vortexed in 2 mL of each solvent to assess solubility, sedimentation or aggregation.

2.8. Optimization of Parameters to Maximize Yield of ZnO NPs

Optimization of physicochemical parameters influencing nanoparticle synthesis was performed using the one-factor-at-a-time (OFAT) method. Each optimized condition was incorporated sequentially into subsequent experiments. For optimization process, the effect of different optical densities (0.2, 0.4, 0.6, 0.8, 1.0 at 540 nm), inoculum size (2%, 4%, 6%, 8%, and 10%), concentrations of $ZnSO_4$ (50–80 mM) and temperature (40°C, and 55°C) was studied. As a standard protocol, isolates were adjusted to 0.2 OD and 2% (v/v) inoculum was added to 10 mM $ZnSO_4$ solution. The flasks were **incubated** at RT for 24 h [18-21].

2.9. Characterization of Synthesized ZnO NPs

The ZnO NPs were characterized based on double-beam UV–Vis spectrophotometry, Fourier Transform Infrared spectroscopy (FTIR), particle size and Scanning Electron Microscope (SEM) analysis. For UV analysis, the NPs were dissolved in 1N HCl and analyzed using 1N HCl as blank. Spectra were scanned between 200–800 nm to identify characteristic absorption peaks at 370–380 nm that confirm ZnO formation [22, 23]. FTIR analysis was conducted at the CIF Department, K.C. College, Churchgate, using a PerkinElmer Spectrum IR spectrometer to identify functional groups associated with ZnO NPs [22, 24]. The size of NPs was analyzed using a HORIBA Nanoparticle Size Analyzer at

Dr. P.S. Ramanathan Advanced Instrumentation Centre, Ramnarain Ruia Autonomous College, Matunga. Samples were ultrasonicated for 15 min prior to measurement. Morphological characterization was performed using SEM at Karmaveer Bhaurao Patil College, Vashi, to observe surface topology and particle distribution.

2.10. Applications of Synthesized ZnO Nanoparticles as Antimicrobial Agent

Antimicrobial potential of ZnO NPs was assessed using the agar well diffusion method against ten bacterial strains including *Escherichia coli*, *Klebsiella pneumoniae*, *Staphylococcus aureus*, *Salmonella typhi*, *S. paratyphi* A, *S. paratyphi* B, *Shigella dysenteriae* var. schmitzii, *Pseudomonas aeruginosa*, *Streptococcus pyogenes*, and *Bacillus subtilis*. For determination of antibacterial activity, a ZnO NP stock (200 mg/mL) was prepared in 1N HCl, sterilized using 0.2 µm filtration, and 50µL volume was added to wells in SDA plates seeded with test cultures. Plates were incubated at 37°C for 24 h. The experiments were performed in triplicates and, after incubation, the inhibition zones were measured and mean diameters were documented after subtracting control values. [25, 26].

2.11. Applications of Synthesized ZnO Nanoparticles in Photocatalytic Degradation of Congo Red Dye

The λmax of Congo red dye was determined by running a spectrum scan between 200 to 800 nm using a UV-Vis spectrophotometer. For the analysis, 1:2 diluted 1mM Congo red dye was prepared and its absorbance was measured at 506nm. For the test system, 1.5ml of diluted Congo red was mixed with 0.01g of synthesized ZnO NP while the control system was devoid of ZnO NP. Four tubes of the test system were prepared along with their individual controls and labelled as 30mins, 60mins, 90mins, and 120mins. Further these systems were exposed to UV light for the respective time intervals (to detect photocatalytic degradation) followed by UV-Vis spectrophotometer analysis at 506nm [27].

3. Result and discussion

3.1. Screening and Isolation

Arriaza-Echanes et al. [28] has emphasized that the NP producing yeasts are widely distributed in soil environments. Similarly, studies have reported NP synthesis capabilities among marine yeasts [29], while sugarcane bagasse serves as a nutrient rich substrate supporting diverse yeast communities [30]. Hence, these samples were collected for isolation of yeast in this study. In total, seven yeast strains were isolated. Among them, two isolates (M1, M2) were obtained from sea water sample, two from rhizospheric soil sample (U1, G1) and 3 from sugarcane bagasse (IQA-1, IQA-2 and IQA-3). Microscopic examination using monochrome staining revealed circular to oval yeast cells measuring approximately 1–2 mm. Some cells were observed in the budding stage.

3.2. Enzymatic Profiling of Isolates

The enzyme activity of the isolates is represented in Table 1. Out of the seven isolates, two marine and two soil-derived isolates showed nitrate reductase and dehydrogenase activity, while these activities were absent in all three isolates obtained from sugarcane bagasse.

Table 1 Enzymatic profile of Isolates

Sr. No.	Yeast isolates	Observation for Nitrate reduction test	Observation for dehydrogenase test	Inference
1.	U1	Red precipitate	Red spot	+
2.	G1	Red precipitate	Red spot	+
3.	M1	Red precipitate	Red spot	+
4.	M1	Red precipitate	Red spot	+
5.	IQA-1	No red precipitate	No red spot	-
6.	IQA-2	No red precipitate	No red spot	-
7.	IQA-3	No red precipitate	No red spot	-

Microbial synthesis of metal NPs often involves key redox enzymes including nitrate reductase and dehydrogenases. Nitrate reductase mediates the reduction of nitrate to nitrite, generating electrons that can subsequently reduce metal ions such as Ag^{+} and Au^{3+} from their respective nitrate precursors [31]. Dehydrogenases, on the other hand, are

members of the oxidoreductase family. They play a vital role in microbial respiration and redox metabolism. These enzymes catalyze electron transfer between substrates and electron acceptors such as NAD^+ or $NADP^+$, and have been implicated in the reduction of metal ions (Au^+, Ag^+, Zn^{2+}) to their metallic forms during NP formation [32]. In addition to these mechanisms, microorganisms utilize alternative biochemical pathways and non-enzymatic processes such as precipitation and bio-mineralization to immobilize and neutralize metal ions [33]. For this reason, although IQA-1, IQA-2 and IQA-3 (isolates obtained from sugarcane bagasse) showed no nitrate reductase and dehydrogenase activity, they were tested for their ability to form ZnO NPs.

3.3. Formation and solubility of ZnO NPs

Among the seven isolates, only IQA-1 successfully produced ZnO NPs (Fig. 1). To standardize the protocol, the MTC of $ZnSO_4$ was determined since microbial synthesis of ZnO NPs is strongly influenced by the organism's tolerance to the zinc precursor salt. It was found to be 60 mM. Hence, the same concentration was used as Zn precursor for preparation of NPs. The protocol used in this study yielded approximately 0.01 g of white ZnO NP powder. It was insoluble in polar (distilled water, methanol, dimethyl sulphoxide, chloroform) as well as non-polar (n-hexane, cyclohexane, diethyl ether, and n-butane) solvents, but was soluble in 1N HCl and 1N NaOH. This observation confirmed the amphoteric nature of he formed NPs [34].

Figure 1 ZnO NP synthesized using IQA-1 isolate

The study further suggested that IQA-1 most probably used non-enzymatic mechanisms, such as those mediated by cell wall functional groups, metabolites or secreted biomolecules. Precisely, the yeast cell walls contain polysaccharides, proteins, and lipids rich in hydroxyl, carboxyl and amine groups. These functional groups can interact electrostatically with metal ions and reduce them even in the absence of active reductase enzymes [35]. These groups may also lead to adsorption and nucleation of NPs [36]. It has been indicated in previous studies that these processes are facilitated by slightly alkaline pH [37]. Additionally, metabolites such as organic acids, phenolics or alcohols released during growth may act as reducing and capping agents [38].

The inability of isolates with nitrate reductase and dehydrogenase activity to produce NPs may be due to production of these enzymes intracellularly or production of enzymes with high substrate specificity [39].

3.4. Identification of potential isolate

The consensus sequence and BLAST analysis is represented in Fig. 2. The assembled consensus sequence after amplification of ~600 bp fragment using ITS1 and ITS4 primers showed 92.737% similarity to *Issatchenkia orientalis* (MN710490). To further validate our findings, a phylogenetic analysis was done to generate maximum likelihood tree (Kimura model, 1000 bootstraps), as represented in Fig. 3. It showed tight clustering of test isolate with *I. orientalis*, and

formed a distinct subclade closely associated with Pichia species. This observation is well supported by previously documented taxonomic relationship between *I. orientalis* and *Pichia kudriavzevii*. These strains are often used synonymously [40]. *I. orientalis* is typically associated with fermented foods [41] and rarely with opportunistic infections [42].

25C112_223_IQA_1
GTTCAGCGGGTATTCCTCCTTGATCGGAGGTGGAGTTGGGTTAAAGTTCGCTGCCCGCCCGCGCGCACACACTA
GTTCGCGCAGACCGGCCCTCGCTTGGAGCCGGGGAAAACACGCCTCCCCGCCCAGGTCGGAAGCTCCGCCCCAA
GAAGGAAACGACGCTCAGACAGGCATGCCCGCCGGAATGCCGGCGGGCCCAATGGGCGTTCAAGAACTCGAGG
ATTCACGAGGGCTGCAATTCACACTAGGTATCGCATTTCGCTGCGCTCTTCATCGATGCGAGAACCAAGAGATC
CGTTGTGGAAAGTTTGGGGGATTTCTCGTGTTTGACGGCCGCGCTGCCAGTTTCGGTGTTTCGCTTCGCCCACGC
AGTGGGGAAAAAGTAATTCACAGTAATGATC

qseqid	sseqid	bitscore	score	qcovs	pident
25C112_223_IQA_1	Issatchenkia_orientalis|MN710490	508	275	87	92.737
25C112_223_IQA_1	Pichia_fermentans|KY104545	366	198	83	86.686
25C112_223_IQA_1	Pichia_garciniae|MW710894	285	154	42	97.041
25C112_223_IQA_1	Pichia_chibodasensis|LN870337	276	149	41	96.951
25C112_223_IQA_1	Pichia_deserticola|AY790539	272	147	41	96.364

Figure 2 Consensus sequence (up) and BLAST analysis (down) of ZnO NPs synthesized using *Issatchenkia orientalis*

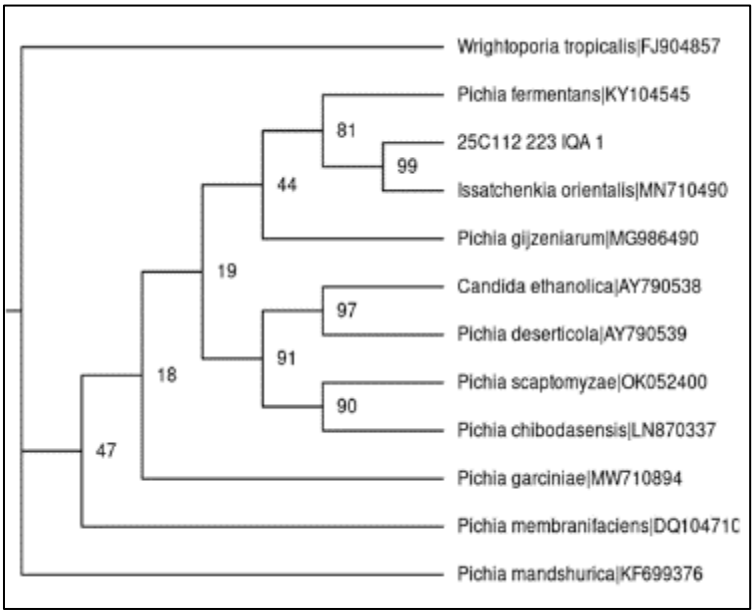

Figure 3 Phylogenetic Tree of *Issatchenkia orientalis*

3.5. Optimization of Nanoparticle Yield

Optimum yield of NPs was obtained at room temperature, when the precursor concentration of 60mM $ZnSO_4$ was mixed with culture density of 0.8 $O.D_{540nm}$ and 6% inoculum size (Fig. 4).

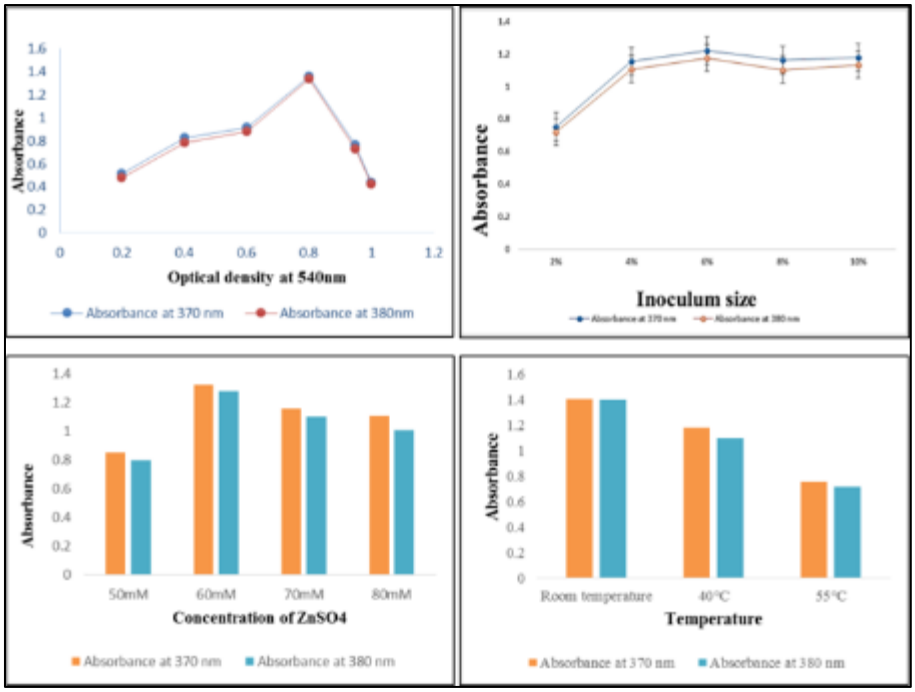

Figure 4 Optimization of Nanoparticle Yield

Multiple optimization studies employing Box–Behnken or RSM approaches have reported that Zn precursor concentration and temperature are the most important factors that control ZnO NP yield [43]. Also, temperature strongly modulates particle morphology and size [44]. In this study, NP yield was maximum at room temperature. This can be explained based on the fact that the microbial enzymatic activity and their metabolic processes are optimum at its physiological growth temperature [45]. Also, the precursor: biomass ratios determine the availability of reducing and capping agents [46]. Hence, depending on the isolate, experimental conditions and precursors used, each study has a unique optimum, beyond which NP yield decreases due to toxicity or substrate depletion. In this study, 60 mM $ZnSO_4$ and 6% inoculum size (0.8 $O.D_{540nm}$) provided the optimum precursor: biomass ratio enabling increased NP yield by 14.28%. In a similar study, 352.4 mM of Zn concentration, pH 9 and 25% of cell-free supernatant volume ratio was reported to be optimum for ZnO NP synthesis using *Lactobacillus plantarum* TA4 [47]. In another study, 60°C and 0.2 M zinc acetate dihydrate was optimum for ZnO NP synthesis using *Leonotis ocymifolia* leaves [48].

3.6. Characterization of ZnO NP

The primary detection and characterization of NPs performed using a double-beam UV–Visible spectrophotometer showed characteristic absorption peaks between 370 nm and 380 nm. The absorption bands correspond to the surface plasmon resonance (SPR) phenomenon, where electron oscillations in the conduction band occur at specific wavelengths. In general, metal oxide NP typically exhibit SPR between 200 nm and 600 nm, while the absorption at 370–380 nm specifically indicates ZnO NP synthesis [11]. Similar peaks have been previously reported by Muhammad et al. [49], Singh et al. [9] and Subha et al. [50].

FT-IR analysis (Fig. 5) revealed an intense band at 562.95 cm^{-1}, attributed to Zn–O stretching vibrations. This observation is consistent with the findings of Abdelhakim et al. [24] and Gatou et al. [51] who reported similar bands between 400–700 cm^{-1}. The bands at 1631.02 cm^{-1} and 3228.30 cm^{-1} corresponded to amide I vibrations of proteins and overlapping hydroxyl group stretching, respectively. Another band observed at 2029.31 cm^{-1} corresponded to amide II and CO_2 vibrations [11, 18]. The presence of these amide groups suggested that microbial proteins were responsible for capping and stabilizing the formed NPs [47].

The particle size was found to be 843.9 nm (Fig. 5), indicating that the formed NPs were large nano-clusters instead of typical NPs [52, 53]. SEM further revealed irregular, non-spherical morphology of ZnO NPs (Fig. 5), consistent with microbial synthesis patterns reported by Kamal et al. [54] and Khairnar et al. [55]. Such irregularity likely resulted from biologically mediated nucleation and growth, producing non-uniform structures that enhance surface area and biological activity. The absence of agglomeration in SEM images further supports the role of microbial biomolecules as natural capping and stabilizing agents.

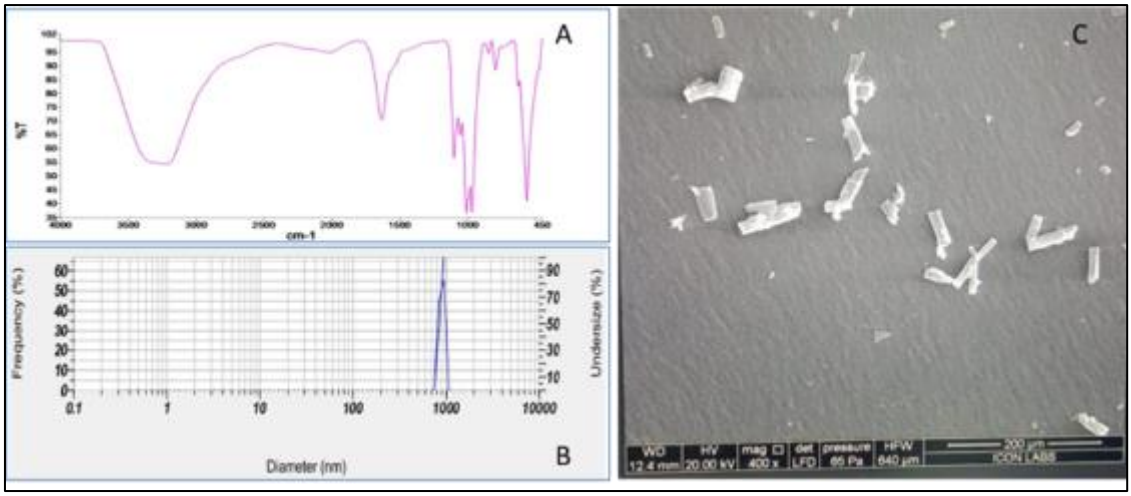

Figure 5 Characterization ZnO NP showing (a) FTIR spectra (b) particle size and (c) SEM image

3.7. Antimicrobial activity of ZnO NPs

The ZnO NPs exhibited moderate antibacterial effects against laboratory isolates, with inhibition zones ranging from 3 to 9 mm (Fig. 6). The highest activity was observed against *Bacillus subtilis*. Similar to our study, Mendes et al. [56] reported significant membrane disruption in *Bacillus subtilis* using ZnO NPs. In contrast, De Souza et al. [25] observed no antibacterial activity of ZnO NPs against *Bacillus* species. Also, contrasting to our observations, Jiang et al. [57] reported high activity of ZnO NPs against *E. coli*. These variations in observation could be due to differences in NP synthesis methods, size, surface charge and concentration [25, 57].

The antibacterial efficacies of biogenic ZnO NPs are significant in the present era of antibiotic resistance. This is because the NPs offer a multifaceted mechanism of action which reduces the likelihood of resistance development. These mechanisms include the generation of reactive oxygen species (ROS), disruption of bacterial cell wall integrity, and the release of Zn^{2+} ions that interfere with vital cellular functions [26].

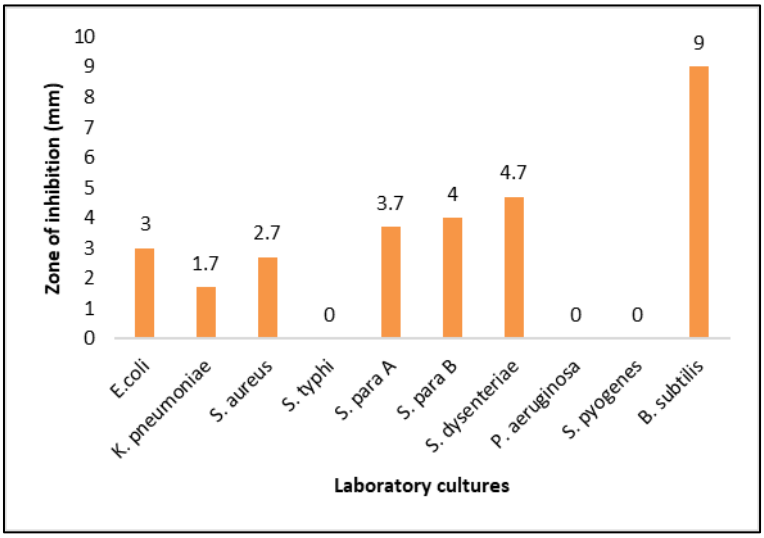

Figure 6 Zone of inhibition of ZnO NP observed against laboratory cultures

3.8. Photocatalytic Degradation of Congo Red Dye by ZnO NPs

Figure 7 illustrates the photocatalytic degradation of Congo red dye over duration of 120 mins under UV light exposure. The initial absorbance of both the control and test samples was recorded as 1.761 at 506 nm. Throughout the experiment, the test sample containing ZnO NPs consistently demonstrated lower absorbance values compared to the control, indicating progressive degradation of the dye. After 120 mins, the absorbance values were 0.798 and 1.098 for the test and control, respectively. The reduction in absorbance in the test sample confirmed the photocatalytic activity

of ZnO NPs under UV irradiation. The degradation efficiency of Congo red dye was calculated to be 54.68%. In comparison, the control sample exposed to UV light alone showed only 37.64% degradation.

Previous studies have reported higher degradation efficiencies under optimized conditions. For instance, Elaziouti et al. [58] achieved 95.02% degradation of Congo red within 60 mins using chemically synthesized ZnO NPs at pH 8. Similarly, Nwaiwu et al. [27] demonstrated 99.7% degradation efficiency using nitrogen and silver-doped ZnO NPs under UV light at pH 8 after 120 mins. These findings emphasize that pH and other parameters play a critical role in determining photocatalytic efficiency of NPs.

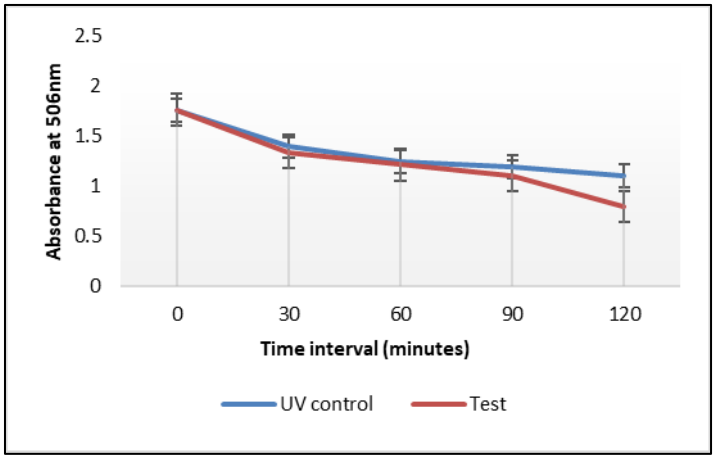

Figure 7 Photocatalytic degradation of Congo red dye under UV light by ZnO NPs

4. Conclusion

The present study demonstrates a sustainable, eco-friendly and biogenic synthesis of ZnO NPs using *I. orientalis*. The biological approaches eliminate the need for high energy inputs, extreme reaction conditions and harsh chemicals. Furthermore, the microbial synthesis process offers inherent biocompatibility, as the biomolecules involved in NP formation act as natural capping and stabilizing agents. This makes the obtained ZnO NPs particularly suitable for applications in biomedical, cosmetic and food-packaging sectors, where safety and sustainability are highly crucial. In addition, the biogenic approach is adaptable and can be optimized for producing a range of metal and metal-oxide NPs. Overall, this study highlight the dual action of microbially-synthesized ZnO NPs for environmental remediation and antimicrobial applications.

Compliance with ethical standards

Disclosure of conflict of interest

No conflict of interest to be disclosed.

References

[1] Burlec AF, Corciova A, Boev M, Batir-Marin D, Mircea C, Cioanca O, Danila G, Danila M, Bucur AF, Hancianu M. Current overview of metal nanoparticles' synthesis, characterization, and biomedical applications, with a focus on silver and gold nanoparticles. Pharmaceuticals. 2023; 16(10):1410.

[2] Abbasi R, Shineh G, Mobaraki M, Doughty S, Tayebi L. Structural parameters of nanoparticles affecting their toxicity for biomedical applications: A review. Journal of nanoparticle research. 2023; 25:43.

[3] Joudeh N, Linke D. Nanoparticle classification, physicochemical properties, characterization, and applications: A comprehensive review for biologists. Journal of nanobiotechnology. 2022; 20(1):1–27.

[4] Khan Y, Sadia H, Shah SZA, Khan MN, Shah AA, Ullah N, Ullah MF, Bibi H, Bafakeeh OT, Khedher NB, Eldin SM, Fadhl BM, Khan MI. Classification, synthetic, and characterization approaches to nanoparticles, and their applications in various fields of nanotechnology: A review. Catalysts. 2022; 12(11):1386.

[5] Vishwanath R, Negi B. Conventional and green methods of synthesis of silver nanoparticles and their antimicrobial properties. Current research in green and sustainable chemistry. 2021; 4:100205.

[6] Gunasena MDKM, Galpaya GDC P, Abeygunawardena CJ, Induranga DKA, Priyadarshana HVV, Millavithanachchi SS, Bandara PKGSS, Koswattage KR. Advancements in bio-nanotechnology: Green synthesis and emerging applications of bio-nanoparticles. Nanomaterials. 2025; 15(7):528.

[7] Singaravelu S, Motsoene F, Abrahamse H, Dhilip Kumar SS. Green-synthesized metal nanoparticles: A promising approach for accelerated wound healing. Frontiers in bioengineering and biotechnology. 2025; 13:1637589.

[8] Abuzeid HM, Julien CM, Zhu L, Hashem AM. Green synthesis of nanoparticles and their energy storage, environmental, and biomedical applications. Crystals. 2023; 13(11):1576.

[9] Singh P, Kim YJ, Singh H, Wang C, Hwang KH, Farh M-AL, Yang DC. Biosynthesis, characterization, and antimicrobial applications of silver nanoparticles. International journal of nanomedicine. 2015; 10:2567–77.

[10] Zhou X-Q, Hayat Z, Zhang D-D, Li M-Y, Hu S, Wu Q, Cao Y-F, Yuan Y. Zinc oxide nanoparticles: Synthesis, characterization, modification, and applications in food and agriculture. Processes. 2023; 11(4):1193.

[11] Jain D, Shivani, Bhojiya AA, Singh H, Daima HK, Singh M, Mohanty SR, Stephen BJ, Singh A. Microbial fabrication of zinc oxide nanoparticles and evaluation of their antimicrobial and photocatalytic properties. Frontiers in chemistry. 2020; 8:778.

[12] Alsamhary KI. Eco-friendly synthesis of silver nanoparticles by *Bacillus subtilis* and their antibacterial activity. Saudi journal of biological sciences. 2020; 27(8):2185–91.

[13] Lebaka VR, Ravi P, Reddy MC, Thummala C, Mandal TK. Zinc oxide nanoparticles in modern science and technology: Multifunctional roles in healthcare, environmental remediation, and industry. Nanomaterials. 2025; 15(10):754.

[14] Al Miad A, Saikat SP, Alam MK, Hossain MS, Bahadur NM, Ahmed S. Metal oxide-based photocatalysts for the efficient degradation of organic pollutants for a sustainable environment: A review. Nanoscale advances. 2024; 6:4781–803.

[15] Smithee S, Tracy S, Drescher KM, Pitz LA, McDonald T. A novel, broadly applicable approach to isolation of fungi in diverse growth media. Journal of microbiological methods. 2014; 105:155–61.

[16] Chauhan R, Reddy A, Abraham J. Biosynthesis of silver and zinc oxide nanoparticles using *Pichia fermentans* JA2 and their antimicrobial property. Applied nanoscience. 2015; 5:63–71.

[17] Schoch CL, Seifert KA, Huhndorf S, Robert V, Spouge JL, Levesque CA, Chen W, Fungal Barcoding Consortium. Nuclear ribosomal internal transcribed spacer (ITS) region as a universal DNA barcode marker for fungi. Proceedings of the national academy of sciences. 2012; 109(16):6241–6.

[18] Ahmad A, Mukherjee P, Senapati S, Mandal D, Khan MI, Kumar R, Sastry M. Extracellular biosynthesis of silver nanoparticles using the fungus *Fusarium oxysporum*. Colloids and surfaces B: biointerfaces. 2003; 28(4):313–18.

[19] Govindappa M, Farheen H, Chandrappa CP, Channabasava, Rai RV, Raghavendra VB. Mycosynthesis of silver nanoparticles using extract of endophytic fungi, *Penicillium* species of *Glycosmis mauritiana*, and its antioxidant, antimicrobial, anti-inflammatory and tyrosinase inhibitory activity. Advances in natural sciences: nanoscience and nanotechnology. 2016; 7(3):035014.

[20] Hulkoti NI, Taranath TC. Biosynthesis of nanoparticles using microbes—a review. Colloids and surfaces B: biointerfaces. 2014; 121:474–83

[21] Sharma A, Singh BP, Dhar S, Gondorf A, Spasova M. Effect of surface groups on the luminescence property of ZnO nanoparticles synthesized by sol-gel route. Surface science. 2012; 606(3–4):L13–L17.

[22] Ijaz I, Gilani E, Nazir A, Bukhari A. Detail review on chemical, physical and green synthesis, classification, characterizations and applications of nanoparticles. Green chemistry letters and reviews. 2020; 13(3):223–45.

[23] Giri PK, Bhattacharyya S, Singh DK, Kesavamoorthy R, Panigrahi BK, Nair KGM. Correlation between microstructure and optical properties of ZnO nanoparticles synthesized by ball milling. Journal of applied physics. 2007; 102(9):093515.

[24] Abdelhakim HK, El-Sayed ER, Rashidi FB. Biosynthesis of zinc oxide nanoparticles with antimicrobial, anticancer, antioxidant and photocatalytic activities by the endophytic Alternaria tenuissima. Journal of applied microbiology. 2020; 128(6):1634–46.

[25] De Souza RC, Haberbeck LU, Riella HG, Ribeiro DHB, Carciofi BAM. Antibacterial activity of zinc oxide nanoparticles synthesized by solochemical process. Brazilian journal of chemical engineering. 2019; 36(2):885–93.

[26] Sirelkhatim A, Mahmud S, Seeni A, Kaus NHM, Ann LC, Bakhori SKM, Hasan H, Mohamad D. Review on zinc oxide nanoparticles: Antibacterial activity and toxicity mechanism. Nano-micro letters. 2015; 7(3):219–42.

[27] Nwaiwu BC, Oguzie EE, Ejiogu CC. Photocatalytic degradation of Congo red using doped zinc oxide nanoparticles. EQA. 2024; 60:18–26.

[28] Arriaza-Echanes C, Campo-Giraldo JL, Valenzuela-Ibaceta F, Ramos-Zúñiga J, Pérez-Donoso JM. Biosynthesis of Cu-In-S nanoparticles by a yeast isolated from Union Glacier, Antarctica: A platform for enhanced quantum dot-sensitized solar cells. Nanomaterials. 2024; 14(6):–.

[29] Basheer MA, Abutaleb K, Abed NN, Mekawey AAI. Mycosynthesis of silver nanoparticles using marine fungi and their antimicrobial activity against pathogenic microorganisms. Journal of genetic engineering and biotechnology. 2023; 21(1):127.

[30] Sidana A, Farooq U. Sugarcane bagasse: A potential medium for fungal cultures. Chinese journal of biology. 2014; 2014:1–5.

[31] Anil Kumar S, Abyaneh MK, Gosavi SW, Kulkarni SK, Pasricha R, Ahmad A, Khan MI. Nitrate reductase-mediated synthesis of silver nanoparticles from $AgNO_3$. Biotechnology letters. 2007; 29(3):439–45.

[32] Porzani SJ, Lorenzi AS, Eghtedari M, Nowruzi B. Interaction of dehydrogenase enzymes with nanoparticles in industrial and medical applications, and the associated challenges: A mini-review. Mini reviews in medicinal chemistry. 2021; 21(11):1351–66.

[33] Bahrulolum H, Nooraei S, Javanshir N, Tarrahimofrad H, Mirbagheri VS, Easton AJ, Ahmadian G. Green synthesis of metal nanoparticles using microorganisms and their application in the agrifood sector. Journal of nanobiotechnology. 2021; 19(1):86.

[34] Siddiqi KS, ur Rahman A, Tajuddin, Husen A. Properties of zinc oxide nanoparticles and their activity against microbes. Nanoscale research letters. 2018; 13:141.

[35] Pan J, Qian H, Sun Y, Miao Y, Zhang J, Li Y. Microbially synthesized nanomaterials: Advances and applications in biomedicine. Precision medicine and engineering. 2025; 2(1):100019.

[36] Kazemi S, Hosseingholian A, Gohari SD, Feirahi F, Moammeri F, Mesbahian G, Moghaddam ZS, Ren Q. Recent advances in green synthesized nanoparticles: From production to application. Materials today sustainability. 2023; 24:100500.

[37] Mikhailova EO. Green silver nanoparticles: An antibacterial mechanism. Antibiotics. 2025; 14(1):5.

[38] Villagrán Z, Anaya-Esparza LM, Velázquez-Carriles CA, Silva-Jara JM, Ruvalcaba-Gómez JM, Aurora-Vigo EF, Rodríguez-Lafitte E, Rodríguez-Barajas N, Balderas-León I, Martínez-Esquivias F. Plant-based extracts as reducing, capping, and stabilizing agents for the green synthesis of inorganic nanoparticles. Resources. 2024; 13(6):70.

[39] Bhatnagar S, Aoyagi H. Current overview of the mechanistic pathways and influence of physicochemical parameters on the microbial synthesis and applications of metallic nanoparticles. Bioprocess and biosystems engineering. 2025; 48(11):1779–800.

[40] Kurtzman CP, Smiley MJ, Johnson CJ. Emendation of the genus Issatchenkia Kudriavzev and comparison of species by deoxyribonucleic acid reassociation, mating reaction, and ascospore ultrastructure. International journal of systematic and evolutionary microbiology. 1980; 30:503–13.

[41] Ongol MP, Asano K. Main microorganisms involved in the fermentation of Ugandan ghee. *Int J Food Microbiol*. 2009; 133:286–91.

[42] Opulente DA, Langdon QK, Buh KV, Haase MAB, Sylvester K, Moriarty RV, Jarzyna M, Considine SL, Schneider RM, Hittinger CT. Pathogenic budding yeasts isolated outside of clinical settings. *FEMS Yeast Res*. 2019; 19(3):foz032.

[43] Mechi L, Chemingui H, Chékir J, Alsukaibi AKD, Azaza H, Mhiri M. Plant mediated green synthesis of zinc oxide nanoparticles for photocatalytic degradation of trypan blue: Optimisation via Box–Behnken design. *Results Chem*. 2025; 18:102822.

[44] Liu H, Zhang H, Wang J, Wei J. Effect of temperature on the size of biosynthesized silver nanoparticles: Deep insight into microscopic kinetics analysis. *Arab J Chem*. 2020; 13(1):1011–19.

[45] Price PB, Sowers T. Temperature dependence of metabolic rates for microbial growth, maintenance, and survival. *Proc Natl Acad Sci USA*. 2004; 101(13):4631–6.

[46] Sharma D, Kanchi S, Bisetty K. Biogenic synthesis of nanoparticles: A review. *Arab J Chem*. 2019; 12(8):3576–600.

[47] Yusof HM, Rahman NA, Mohamad R, Zaidan UH, Samsudin AA. Optimization of biosynthesis zinc oxide nanoparticles: Desirability-function based response surface methodology, physicochemical characteristics, and its antioxidant properties. *OpenNano*. 2022; 8:100106.

[48] Mutukwa D, Taziwa RT, Tichapondwa SM, Khotseng L. Optimisation, synthesis, and characterisation of ZnO nanoparticles using *Leonotis ocymifolia* leaf extracts for antibacterial and photodegradation applications. *Int J Mol Sci*. 2024; 25(21):11621.

[49] Muhammad W, Ullah N, Haroon M, Abbasi BH. Optical, morphological and biological analysis of zinc oxide nanoparticles (ZnO NPs) using *Papaver somniferum* L. *RSC Adv*. 2019; 9(51):29541–8.

[50] Subba B, Rai GB, Bhandary R, Parajuli P, Thapa N, Kandel DR, Mulmi S, Shrestha S, Malla S. Antifungal activity of zinc oxide nanoparticles (ZnO NPs) on *Fusarium equiseti* phytopathogen isolated from tomato plant in Nepal. *Heliyon*. 2024; 10(22):e40198.

[51] Gatou M-A, Lagopati N, Vagena I-A, Gazouli M, Pavlatou EA. ZnO nanoparticles from different precursors and their photocatalytic potential for biomedical use. *Nanomaterials*. 2023; 13(1):122.

[52] Sharon M, Sharon M, Pandey S, Oza G. *Bio-Nanotechnology*. Ane Books Pvt. Ltd. for CRC Press Taylor & Francis Group: New Delhi, India; 2012.

[53] Poole CP, Owens FJ. *Introduction to Nanoscience and Nanotechnology*. 1st ed. Wiley India Pvt. Ltd.: New Delhi, India; 2021.

[54] Kamal A, Saba M, Kamal A, Batool M, Asif M, Al-Mohaimeed AM, Al Farraj DA, Habib D, Ahmad S. Bioinspired green synthesis of bimetallic iron and zinc oxide nanoparticles using mushroom extract and use against *Aspergillus niger*. *Catalysts*. 2023; 13(2):400.

[55] Khairnar N, Kwon H, Park S, Lee H, Park J. Tailoring the size and shape of ZnO nanoparticles for enhanced performance of OLED device. *Nanomaterials*. 2023; 13(21):2816.

[56] Mendes CR, Dilarri G, Forsan CF, Sapata VMR, Lopes PRM, de Moraes PB, Montagnolli RN, Ferreira H, Bidoia ED. Antibacterial action and target mechanisms of zinc oxide nanoparticles against bacterial pathogens. *Sci Rep*. 2022; 12(1):6657.

[57] Jiang Y, Zhang L, Wen D, Ding Y. Role of physical and chemical interactions in the antibacterial behavior of ZnO nanoparticles against *E. coli*. *Mater Sci Eng C*. 2016; 69:1361–6.

[58] Laouedj N, Abdelkader E, Ahmed B. Photodegradation study of Congo Red in aqueous solution using ZnO/UV-A: Effect of pH and band gap of other semiconductor groups. *J Chem Eng Process Technol*. 2011; 2(2):1000108.